3D Flowerlike Ceria Micro/Nanocomposite Structure and Its Application for Water Treatment and CO Removal

Liang-Shu Zhong,† Jin-Song Hu, An-Min Cao, Qiang Liu,† Wei-Guo Song, and Li-Jun Wan*

Beijing National Laboratory for Molecular Sciences, Institute of Chemistry, Chinese Academy of Sciences (CAS), Beijing 100080, China

Received October 16, 2006. Revised Manuscript Received December 24, 2006

A simple and economical route based on ethylene glycol mediated process was developed to synthesize three-dimensional (3D) flowerlike ceria micro/nanocomposite structure using cerium chloride as a reactant. Scanning electron microscopy (SEM) and X-ray diffraction (XRD) were adopted to investigate the evolution process of ceria precursor, and a two-stage growth process was identified during the morphology evolution. Ceria with the same flowerlike micro/nanocomposite structure was readily obtained by calcination of the ceria precursor. This novel micro/nanocomposite structure held the advantages of both microstructure and nanostructure. Therefore, the as-obtained ceria can be used as not only an effective sorbent for the removal of pollutants in water treatment but also as an excellent support for gold nanoparticles to remove CO by catalytic oxidation, demonstrating a promising potential in environmental remediation.

Introduction

Environmental problems such as air pollution, water pollution, and excessive natural resource consumption represent some of the most formidable challenges facing global society. The development of nanoscience and nanotechnology is expected to play an important role for the remediation of environmental problems. The design and application of novel nanomaterials for environmental protection have been receiving more and more attention in the past few decades. A variety of nanomaterials have been adopted for the treatment of pollutants in the environment. For instance, semiconductor nanomaterials that are activated by light, such as titanium dioxide (TiO_2) and zinc sulfide (ZnS), have been utilized to remove organic contaminants from various contaminated sources.[1,2] Other examples of environmental application of nanomaterials include using zerovalent iron (Fe(0)) and bimetallic Fe(0) nanoparticles as effective redox media for in-situ remediation of organic and inorganic pollutants.[3,4] However, the industrial application of nanomaterials in environmental remediation is limited by availability and cost. One of the ultimate goals of nanoscience and nanotechnology for environmental application is to develop simple and economical routes for designing novel nanomaterials which can efficiently remove various contaminants in the environment and can be easily recovered and reused for many times.

As a typical kind of rare earth oxide, ceria has been the subject of intense interest because of its unique properties, including oxygen storage capacity[5] and oxygen ion conductivity.[6] Because of these characteristics, ceria has been widely used for catalyst,[7] fuel cell,[8] sensor,[9] UV shielding,[10] and luminescence.[11] Ceria has also been used as an important abrasive nanomaterial for chemical−mechanical planarization (CMP) of advanced integrated circuits[12] and as a sulfur sorbent for the removal of H_2S from hot fuel gas streams.[13] For nanometer-sized ceria, the corresponding size-induced property changes, such as catalytic activity,[14] blue shift of absorption spectra,[15] lattice expansion,[16] and phase transformation,[17] are obvious and cannot be ignored. For example, hierarchically mesostructured ceria exhibits a photovoltaic response, while normal ceria does not show this response.[14] Thus, it is urgent to design functional ceria materials with certain size and shape by simple morphology controllable routes. In the past few years, well-defined ceria nanostruc-

* To whom correspondence should be addressed. Tel. & Fax: (+86)10-62558934. E-mail: wanlijun@iccas.ac.cn.

† Also in Graduate School of CAS, Beijing, China.

(1) Linsebigler, A. L.; Lu, G. Q.; Yates, J. T. *Chem. Rev.* **1995**, *95*, 735.
(2) Hu, J. S.; Ren, L. L.; Guo, Y. G.; Liang, H. P.; Cao, A. M.; Wan, L. J.; Bai, C. L. *Angew. Chem., Int. Ed.* **2005**, *44*, 1269.
(3) Zhang, Y. W.; Si, R.; Liao, C. S.; Yan, C. H. *J. Phys. Chem. B* **2003**, *107*, 10159.
(4) Bang, S.; Korfiatis, G. P.; Meng, X. G. *J. Hazard. Mater.* **2005**, *121*, 61.
(5) Trovarelli, A. *Catal. Rev. Sci. Eng.* **1996**, *38*, 439.
(6) Inaba, H.; Tagawa, H. *Solid State Ionics* **1996**, *83*, 1.
(7) Trovarelli, A.; de Leitenburg, C.; Boaro, M.; Dolcetti, G. *Catal. Today* **1999**, *50*, 353.
(8) Park, S. D.; Vohs, J. M.; Gorte, R. J. *Nature* **2000**, *404*, 265.
(9) Brosha, E. L.; Mukundan, R.; Brown, D. R.; Garzon, F. H.; Visser, J. H. *Solid State Ionics* **2002**, *148*, 61.
(10) Yabe, S.; Sato, T. *J. Solid State Chem.* **2003**, *171*, 7.
(11) Fujihara, S.; Oikawa, M. *J. Appl. Phys.* **2004**, *95*, 8002.
(12) Feng, X. D.; Sayle, D. C.; Wang, Z. L.; Paras, M. S.; Santora, B.; Sutorik, A. C.; Sayle, T. X. T.; Yang, Y.; Ding, Y.; Wang, X. D.; Her, Y. S. *Science* **2006**, *312*, 1504.
(13) Flytzani-Stephanopoulos, M.; Sakbodin, M.; Wang, Z. *Science* **2006**, *312*, 1508.
(14) Carrettin, S.; Concepcion, P.; Corma, A.; Nieto, J. M. L.; Puntes, V. F. *Angew. Chem., Int. Ed.* **2004**, *43*, 2538.
(15) Tsunekawa, S.; Fukuda, T.; Kasuya, A. *J. Appl. Phys.* **2000**, *87*, 1318.
(16) Tsunekawa, S.; Ishikawa, K.; Li, Z. Q.; Kawazoe, Y.; Kasuya, A. *Phys. Rev. Lett.* **2000**, *85*, 3440.
(17) Wang, Z. W.; Saxena, S. K.; Pischedda, V.; Liermann, H. P.; Zha, C. S. *Phys. Rev. B* **2001**, *6401*.

10.1021/cm062471b CCC: $37.00
Published on Web 03/01/2007

tures with various morphology such as nanoparticles,[18] nanorods,[19] nanowires,[20] nanotubes,[21] and nanopolyhedrons[22] have been successfully fabricated by a variety of methods. Recently, Sun et al. prepared monodispersed flowerlike CeO_2 microspheres for ethanol steam reforming by a novel hydrothermal method.[23] However, there are few reports on three-dimensional (3D) ceria micro/nanocomposite structure. 3D micro/nanocomposite structure is composed of nanosized building blocks hierarchically while the total size is in micrometer scale. Such a hierarchical structure with the cooperation of microstructure and nanostructure provides a novel approach to bring forth new properties.[24,25] Because of the distinct size, shape, and chemical functionality, 3D ceria micro/nanocomposite structure possesses the advantages from microstructure and nanostructure and can be a promising candidate for many applications. Obviously, it is highly desirable to develop novel and smart synthetic procedures for building 3D ceria micro/nanocomposite structure.

Ethylene glycol mediated process has been successfully adopted to synthesize various metal alkoxide and metal oxide nanomaterials.[26−31] Herein, we further extended this synthetic method to produce uniform-sized ceria nanomaterial with 3D flowerlike micro/nanocomposite structure. Using cerium chloride as the metal ion source, we had successfully synthesized ceria precursor with 3D flowerlike micro/nanocomposite structure which could be calcined into crystalline ceria without changing its original morphology. The as-prepared ceria with 3D flowerlike micro/nanocomposite structure held the advantages of both microstructure and nanostructure. The main advantages that make it particularly attractive for environmental remediation and other applications are in that (1) separation and recycle are easier compared with common nanoparticles as the total size of the structure is in micrometer scale; (2) the as-obtained CeO_2 still keeps high specific surface area as the micropetal of the composite structure is made up of interconnected nanoparticles; (3) the flowerlike structure can effectively prevent further aggregation, so unblocked mass transfer and high catalytic activity can be retained. In this report, we demonstrated that the as-prepared ceria nanomaterial could be used as a sorbent for the removal of As(V) and Cr(VI) in wastewater treatment. This new sorbent could be recovered and reused easily because of its novel structure. In addition, it could also be used as a support for Au nanoparticles to remove CO efficiently by catalytic oxidation with high activity and durability.

(18) Yin, L. X.; Wang, Y. Q.; Pang, G. S.; Koltypin, Y.; Gedanken, A. *J. Colloid Interface Sci.* **2002**, *246*, 78.
(19) Huang, P. X.; Wu, F.; Zhu, B. L.; Gao, X. P.; Zhu, H. Y.; Yan, T. Y.; Huang, W. P.; Wu, S. H.; Song, D. Y. *J. Phys. Chem. B* **2005**, *109*, 19169.
(20) Yu, T. Y.; Joo, J.; Park, Y. I.; Hyeon, T. *Angew. Chem., Int. Ed.* **2005**, *44*, 7411.
(21) Tang, C. C.; Bando, Y.; Liu, B. D.; Golberg, D. *Adv. Mater.* **2005**, *17*, 3005.
(22) Si, R.; Zhang, Y. W.; You, L. P.; Yan, C. H. *Angew. Chem., Int.* Ed. **2005**, *44*, 3256.
(23) Sun, C. W.; Sun, J.; Xiao, G. L.; Zhang, H. R.; Qiu, X. P.; Li, H.; Chen, L. Q. *J. Phys. Chem. B* **2006**, *110*, 13445.
(24) Feng, L.; Li, S. H.; Li, Y. S.; Li, H. J.; Zhang, L. J.; Zhai, J.; Song, Y. L.; Liu, B. Q.; Jiang, L.; Zhu, D. B. *Adv. Mater.* **2002**, *14*, 1857.
(25) Zhao, Y.; Zhai, J.; Tan, S. X.; Wang, L. F.; Jiang, L.; Zhu, D. B. *Nanotechnology* **2006**, *17*, 2090.
(26) Cao, A. M.; Hu, J. S.; Liang, H. P.; Wan, L. J. *Angew. Chem., Int. Ed.* **2005**, *44*, 4391.
(27) Jiang, X. C.; Wang, Y. L.; Herricks, T.; Xia, Y. N. *J. Mater. Chem.* **2004**, *14*, 695.
(28) Wang, Y. L.; Jiang, X. C.; Xia, Y. N. *J. Am. Chem. Soc.* **2003**, *125*, 16176.
(29) Chakroune, N.; Viau, G.; Ammar, S.; Jouini, N.; Gredin, P.; Vaulay, M. J.; Fievet, F. *New J. Chem.* **2005**, *29*, 355.
(30) Zhong, L. S.; Hu, J. S.; Liang, H. P.; Cao, A. M.; Song, W. G.; Wan, L. J. *Adv. Mater.* **2006**, *18*, 2826.
(31) Cao, A. M.; Hu, J. S.; Liang, H. P.; Song, W. G.; Wan, L. J.; He, X. L.; Gao, X. G.; Xia, S. H. *J. Phys. Chem. B* **2006**, *110*, 15858.

Experimental Section

Preparation of Ceria Precursor and Ceria. All the chemicals here were received from Beijing Chemicals Co. (Beijing, China) without further purification. In a typical procedure, 1.5 g $CeCl_3 \cdot 6H_2O$, 2.2 g urea and 6 g tetrabutylammonium bromide (TBAB) were added to 150 mL ethylene glycol in a 250-mL round flask. The obtained solution was stirred with a magnetic stir bar and was heated to 180 °C. About 30 min later, the reaction was stopped and the mixture was cooled to room temperature. The precipitate was collected as ceria precursor by centrifugation and was washed with ethanol four times. Ceria was from the as-prepared precursor via calcinations in air at 450 °C for 2 h.

Preparation of Ceria-Supported Gold Catalyst. Au was deposited on the as-obtained ceria support by the following procedure: 0.04 g $HAuCl_4 \cdot 5H_2O$ was added to 5 mL deionized water and the pH value was brought to 10 by the addition of 0.2 M NaOH. The solution was added to the slurry containing 0.3 g of as-obtained ceria in water (6 mL). The pH of the mixing solution was adjusted to 10 with 0.2 M NaOH. After the suspension was stirred overnight at room temperature, the solid was isolated by centrifugation and was washed with deionized water until no chloride ions were detected by the $AgNO_3$ test and then was dried at 100 °C overnight.

Characterization. The products were characterized by scanning electron microscope (SEM, Hitachi S-4300F), transmission electron microscopy (TEM, JEM JEOL 2010), X-ray powder diffraction (XRD, Rigaku D/max-2500 diffractometer with Cu Kα radiation, $\lambda = 0.1542$ nm, 40 kV, 100 mA), and BET (Micrometrics ASAP 2020).

Water Treatment Experiment. Solutions containing different concentrations of As(V) or Cr(VI) were prepared using $Na_3AsO_4 \cdot 12H_2O$ and $K_2Cr_2O_7$ as the sources of As(V) and Cr(VI). The pH value was adjusted to 3 by HCl or NaOH. Then, 0.02 g as-prepared ceria was added to 10 mL of the above solution under stirring. After stirring for a certain time at room temperature, solid and liquid were separated and inductively coupled plasma-optical emission spectroscopy (Optima 5300DV) was used to measure the arsenic or chromium concentration in the remaining solution.

CO Removal Test. CO removal test was performed in a conventional quartz reactor (6.7 mm in outer diameter) with the feeding of 50 mg as-prepared CeO_2 or Au/CeO_2 sample diluted with 0.5 g sea sand. The catalyst was activated in a flow of air (25 mL min^{-1}) at 300 °C for 1 h and then was kept in the desired temperature under the flow of the reactant gas mixture (0.5% CO, 10% O_2, balanced with N_2) with a rate of 50 mL min^{-1}. The composition of the gas was monitored by online gas chromatography (Shimadzu, GC-14C).

Results and Discussion

In a typical procedure, cerium chloride ($CeCl_3 \cdot 6H_2O$), urea, and tetrabutylammonium bromide (TBAB) were dissolved in ethylene glycol (EG). The solution was heated to 180 °C using an oil bath under magnetic stirring and then

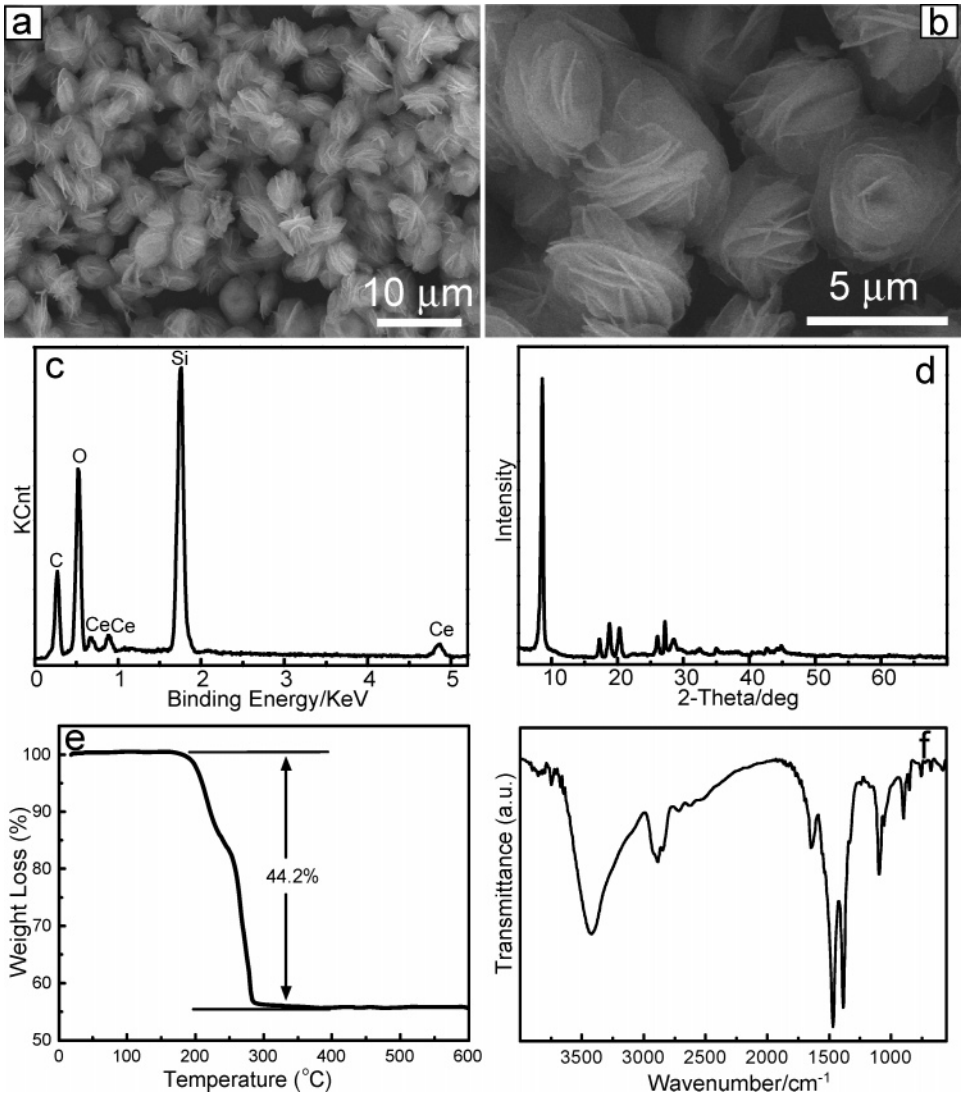

Figure 1. (a) Low-magnification and (b) high-magnification SEM images of the as-prepared ceria precursor. (c) EDX analysis, (d) XRD pattern, (e) TG analysis, and (f) IR spectrum of the as-prepared ceria precursor.

was kept for 30 min. After cooling to room temperature, the as-synthesized precipitate was collected as ceria precursor by four centrifugation and ethanol washing cycles. Scanning electron microscopy (SEM) image of the as-prepared ceria precursor reveals many uniform flowerlike architectures with a diameter varying from 4 to 6 μm (Figure 1a). A closer examination by SEM indicates the entire structure of the architecture was built from micropetals which connected with each other forming the cured 3D flowerlike micro/nano-structure by self-assembly (Figure 1b). A series of other measurements were also used to investigate the as-obtained ceria precursor. Result of the energy-disperse X-ray (EDX) analysis (Figure 1c) confirms that the flowerlike ceria precursor consisted of carbon, cerium, and oxygen, a chemical composition that agreed well with the cerium alkoxide. The powder X-ray diffraction (XRD) pattern of the ceria precursor (Figure 1d) shows a strong low-angle reflection related to interlayer spacing in lamellar structure which was characteristic of stacked metal−oxygen sheets separated by bonded alcoholate anions.[32] If the crystal structure of the precursor was considered as a layered brucite structure in the hexagonal system, the peaks at 8.6°, 17.3°, and 26.0° could be indexed as (001), (002), and (003) reflections, respectively.[29] The interlayer spacing deduced from the positions of these three (00*l*) peaks was 1.034 nm. The (001) peak was rather narrow, revealing a large correlation length along this direction. The mean crystallite size calculated from Scherrer's formula with the full width at half-height (fwhh) of the (001) peak was 22 nm. From thermogravimetric (TG) analysis (Figure 1e), a total weight loss of ∼44.2% was observed in the temperature range from 170 to 300 °C because of the removal of organic species in the precursor by pyrolysis. In the infrared (IR) spectroscopic spectrum of the precursor (Figure 1f), absorption peaks in the range of 2850∼2950 cm^{-1} corresponding to υ_{as} and υ_{s} (C−H) bands, and in the range of 1050∼1125 cm^{-1} corresponding to $\rho(CH_2)$, υ(C−O), and υ(C−C) bands,[29] are observed. X-ray photoelectron spectroscopy (XPS) study of Ce 3d electron core level is characterized by two series of peaks: $3d_{5/2}$ and $3d_{3/2}$.[33,34] For $3d_{5/2}$ of Ce(IV), a mixing of

(32) Larcher, D.; Sudant, G.; Patrice, R.; Tarascon, J. M. *Chem. Mater.* **2003**, *15*, 3543.

(33) Ho, C. M.; Yu, J. C.; Kwong, T.; Mak, A. C.; Lai, S. Y. *Chem. Mater.* **2005**, *17*, 4514.

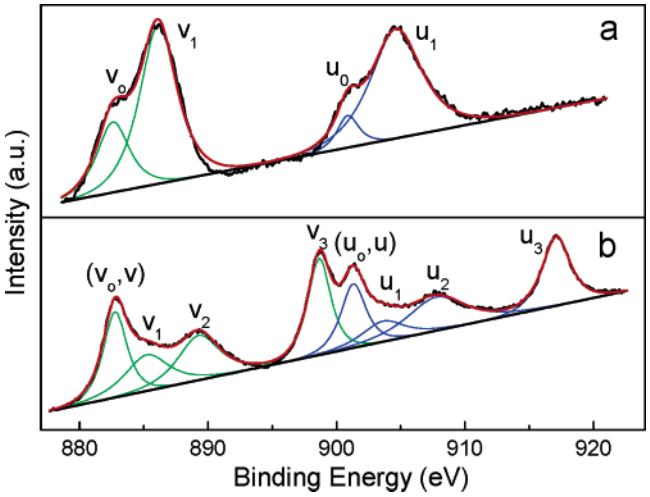

Figure 2. XPS analysis of the Ce 3d states of the as-prepared ceria precursor (a) and ceria (b).

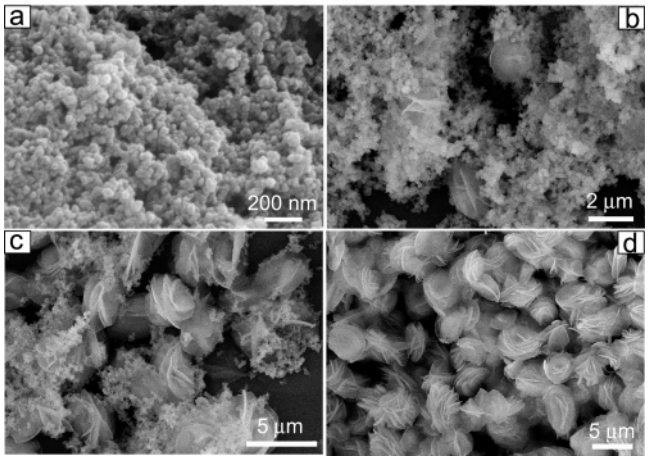

Figure 3. SEM images of the as-prepared ceria precursors collected at different intervals since the precipitate occurred: (a) 3 min, (b) 11 min, (c) 19 min, and (d) 30 min.

the Ce $3d^94f^2L^{n-2}$ and Ce $3d^94f^1L^{n-1}$ states produces the peaks labeled v and v_2, and the Ce $3d^94f^oL^n$ final state forms the peak v_3. For $3d_{5/2}$ of Ce(III), the Ce $3d^94f^2L^{n-1}$ and Ce $3d^94f^1L^n$ states correspond to peaks v_o and v_1. For Ce $3d_{3/2}$ level with the u structure, the same assignment can be carried out. As shown by Figure 2a, only v_o, v_1, u_o, and u_1 could be seen in the Ce 3d XPS spectra of the ceria precursor, which indicated that the oxidation state of cerium was from Ce(III). The above characteristics of the ceria precursor from the different measurements are consistent with those of the reported metallic alkoxide in ethylene glycol mediated process.[26−28,30,31] Thus, it can be concluded that the as-synthesized ceria precursor is cerium alkoxide.

To reveal the formation process of 3D flowerlike micro/nanocomposite structure, samples collected at different intervals from the reaction mixture once the precipitate appeared in the clear solution were investigated by SEM. As shown in Figure 3a, at the early stage, the sample was totally composed of nanoparticles (ca. 100 nm). Figure 3b is an SEM view of the sample collected 11 min later, showing the coexistence of nanoparticles and flowerlike

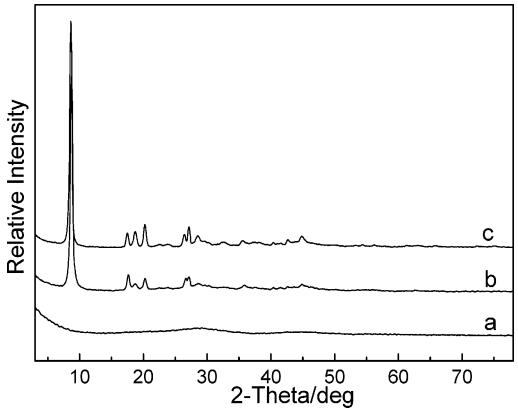

Figure 4. XRD patterns of the as-prepared ceria precursors collected at different intervals since the precipitate occurred: (a) 3 min, (b) 11 min, and (c) 30 min.

micro/nanostructure. As the reaction proceeded, the ratio of the flowerlike micro/nanostructure increased at the expense of the nanoparticles (Figure 3c). At the end, no nanoparticles existed and the sample was all 3D flowerlike micro/nanostructure as shown in Figure 3d. Figure 4 shows the XRD patterns of the samples obtained from different stages. The pattern of the sample collected at the early stage presented no obvious peak (Figure 4a), characteristic of a very poorly crystallized compound. However, the intensity of the peaks of the samples collected later was rather strong (Figure 4b, 4c), which implied that the phase had gradually changed from amorphous to highly crystalline. Amorphous-to-crystalline phase transformation is common in kinetically controlled systems which involves an initial fast-growing amorphous phase and a slow crystallization.[35−37] This morphology evolution process and the corresponding phase transformation in our experiment were similar with previous reports of so-called two-stage growth process which involved a fast nucleation of amorphous primary particles followed by the aggregation and crystallization of primary particles.[38−41] In a control experiment, without the addition of surfactant, we failed to obtain the uniform 3D flowerlike micro/nanocomposite structure. For the products prepared in the absence of TBAB (Figure S1, in Supporting Information), most of the petals could not assemble into 3D flowerlike structure. Therefore, it can be assumed that TBAB molecules facilitate the assembly of petals into the 3D flowerlike structure through the interaction among TBAB molecules and the petals, similar with the cases in the reported literature.[36,37] However, crystallization, electrostatic association with the aggregates, van der Waals force, hydrophobic interaction, and hydrogen bond may be also contributed to the final structure formation.[35−37] The detailed mechanism for the final structure by assembling primary particles is still a puzzle in nanomaterial research.

(34) Nelson, A. E.; Schulz, K. H. *Appl. Surf. Sci.* **2003**, *210*, 206.
(35) Politi, Y.; Arad, T.; Klein, E.; Weiner, S.; Addadi, L. *Science* **2004**, *306*, 1161.
(36) Colfen, H.; Antonietti, M. *Angew. Chem., Int. Ed.* **2005**, *44*, 5576.
(37) Colfen, H.; Mann, S. *Angew. Chem., Int. Ed.* **2003**, *42*, 2350.
(38) Burda, C.; Chen, X. B.; Narayanan, R.; El-Sayed, M. A. *Chem. Rev.* **2005**, *105*, 1025.
(39) Cheng, Y.; Wang, Y. S.; Zheng, Y. H.; Qin, Y. *J. Phys. Chem. B* **2005**, *109*, 11548.
(40) Penn, R. L. *J. Phys. Chem. B* **2004**, *108*, 12707.
(41) Park, J.; Privman, V.; Matijevic, E. *J. Phys. Chem. B* **2001**, *105*, 11630.

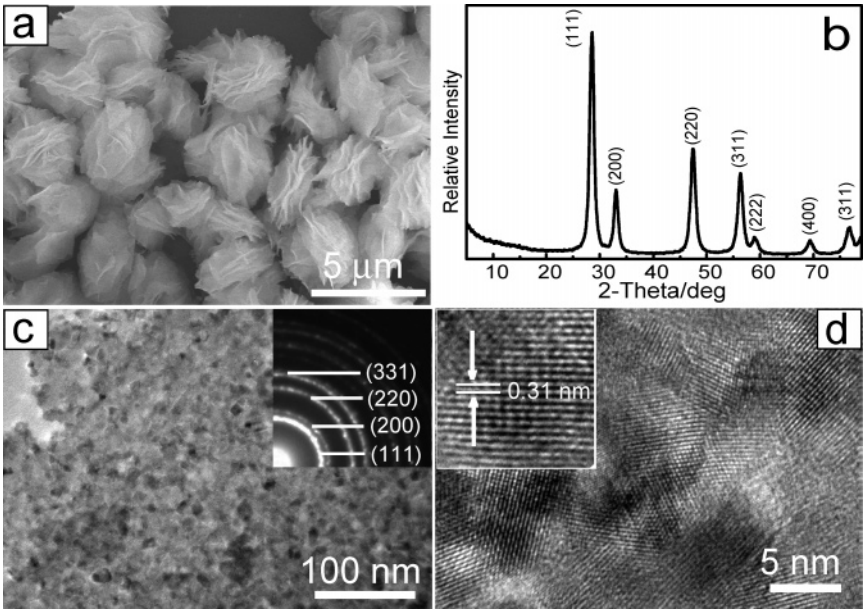

Figure 5. (a) SEM image and (b) XRD pattern of the as-obtained ceria. (c) TEM image of the petal of the flowerlike structure of the as-obtained ceria. The inset was the SAED pattern of the as-obtained ceria. (d) High-resolution TEM (HRTEM) image of the as-obtained ceria. The inset was a magnified HRTEM image.

The addition of urea was found to be very critical in the preparation of flowerlike micro/nanostructure ceria precursor. In a control experiment, when no urea was added under the same reaction conditions, no apparent precipitate was collected. In our experiment, when ethylene glycol deprotonated and coordinated with $CeCl_3$ to form cerium alkoxide, HCl was generated as reported in the reaction between ethylene glycol and metal chloride.[30,42] If HCl was not removed, the accumulation of HCl would inhibit further cerium alkoxide formation. Urea has been adopted to supply steadily OH^- ion through urea hydrolysis.[43−46] When urea was added, the OH^- formed by urea hydrolysis under heating condition would neutralize the HCl and promote the coordination reaction between ethylene glycol and $CeCl_3$, thereby obtaining the ceria precursor.

After the synthesis of the ceria precursor, the effect of calcination on the crystallization and morphology of the product was investigated. Figure 5a shows the SEM image of the calcined product which implied that calcination did not change the total flowerlike morphology of the precursor. The XRD pattern (Figure 5b) reveals that the as-obtained sample after calcination was made of pure CeO_2 (JCPDS Card No. 75-0120) with an average grain size of ca. 11 nm calculated from the width of diffraction peaks using Scherrer's formula. In the lower angle region, the peaks from (001), (002), and (003) reflections of the ceria precursor could not be seen, indicating that the lamellar structure of the precursor disappeared during thermal calcination. Transmission electron microscopy (TEM) image (Figure 5c) indicates that each piece of petal of the flowerlike structure has been transformed from a dense structure with a smooth surface into a highly porous structure consisting of interconnected nanoparticles of 10∼20 nm in size. Selected-area electron diffraction (SEAD) pattern (inset Figure 5c) also confirms that the calcined sample was composed of CeO_2 with a high polycrystalline structure. A representative high-resolution TEM (HRTEM) image taken from the ceria nanoparticles is shown in Figure 5d, which also clearly indicates the polycrystalline characteristic. The lattice fringes are clearly visible with a spacing of 0.31 nm (inset Figure 5d), corresponding to the spacing of the (111) planes of ceria. The XPS spectrum of the calcined sample for Ce 3d states (Figure 2b) was typical of the pure CeO_2.[33,47] Compared with that of the precursor (Figure 2a), the sharp decrease in u_1 and v_1 peaks and the increase of other Ce(IV) peaks indicated that Ce(III) in the precursor had been converted to Ce(IV) as the final oxidation state. Thus, simply by calcination of the as-prepared ceria precursor, we could easily obtain ceria with flowerlike micro/nanocomposite structure. This structure was built from micropetals (ca. 2 μm) while these micropetals were made up of interconnected nanoparticles (10∼20 nm). Obviously, such a novel micro/nanocomposite structure had the features and advantages of both microstructure and nanostructure, and we believed it would have great potential application in many areas.

Ceria is widely used in many different application areas owing to its outstanding physical and chemical properties. As far as environmental remediation is concerned, the main applications of ceria focus on the depollution of gaseous noxious compounds from automobiles and industrial productions (such as removal of SO_x and three-way catalytic treatment of exhaust gases) and the removal of organic compound from wastewater through oxidation (catalytic wet oxidation CWO).[7] Recently, Peng and co-workers showed that the CeO_2−CNT nanomaterials were effective sorbents

(42) Zhang, G.; Liu, M. *J. Mater. Sci.* **1999**, *34*, 3213.
(43) Suber, L.; Sondi, I.; Matijevic, E.; Goia, D. V. *J. Colloid Interface Sci.* **2005**, *288*, 489.
(44) Elyassi, B.; Rajabbeigi, N.; Khodadadi, A.; Mohajerzadeh, S. S.; Sahimi, M. *Sens. Actuators, B* **2004**, *103*, 178.
(45) Hirano, M.; Morikawa, H. *Chem. Mater.* **2003**, *15*, 2561.
(46) Yan, C. L.; Xue, D. F. *J. Phys. Chem. B* **2005**, *109*, 12358.
(47) Venezia, A. M.; Pantaleo, G.; Longo, A.; Di Carlo, G.; Casaletto, M. P.; Liotta, F. L.; Deganello, G. *J. Phys. Chem. B* **2005**, *109*, 2821.

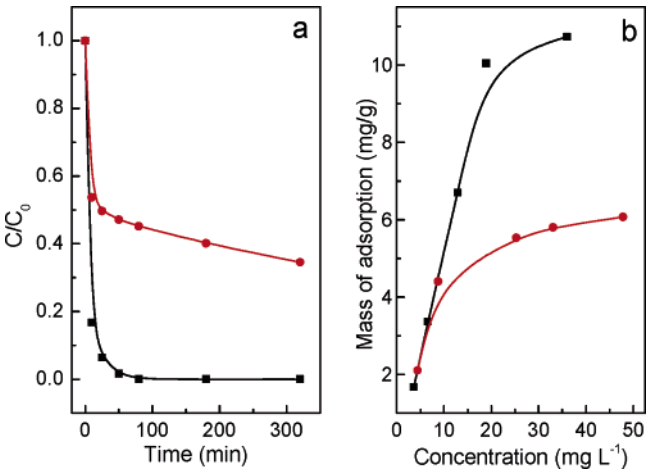

Figure 6. (a) Adsorption rate of As(V) (black line, initial concentration of 12.9 mg g^{-1}) and Cr(VI) (red line, initial concentration of 17.2 mg g^{-1}) on the as-prepared ceria. (b) Adsorption isotherms of As(V) (black line) and Cr(VI) (red line) on the as-prepared ceria.

for As(V) and Cr(VI).[48,49] In these applications, ceria was usually used in the form of nanoparticles for high specific surface area and activity. However, ceria nanoparticles are rather difficult to be handled and be recovered after their applications. Prompted by the novel 3D hierarchical and micro/nanocomposite structure, we expected that the as-obtained ceria nanomaterial in our experiment would be useful in environmental remediation as it had the advantage of easier separation and recycling in practical application compared with ceria nanoparticles. Herein, as a demonstration of potential application, the as-prepared ceria was used as a sorbent for the removal of As(V) and Cr(VI) in wastewater. In addition, it was also adopted as a support for gold nanoparticles, and the as-obtained Au/CeO_2 catalyst was tested for CO oxidation. Both of the above application results suggested that the as-prepared ceria could be a promising material for environmental application.

Arsenic (As) and chromium (Cr) are considered as primary high toxic pollutants in water resource and their efficient removal is considered of great importance. Figure 6a shows the bulk-phase As(V) and Cr(VI) concentration decay lines when 0.05 g of the as-obtained ceria was added to 25 mL As(V) or Cr(VI) solution at room temperature (ca. 25 °C). It is clear from Figure 6a that the adsorption rate was rather fast. In such experiment condition, most of the As(V) and Cr(VI) could be removed after 5 h, and the removal capacity of ceria for As(V) and Cr(VI) was measured to be 6.7 mg g^{-1} and 5.8 mg g^{-1}, respectively. The mechanism for the adsorption was thought to be the affinity between the surface of ceria and the As(V) or Cr(VI) anions by ion exchange.[48,49] The adsorption isotherms of As(V) and Cr(VI) by the as-prepared ceria at different initial concentrations are illustrated in Figure 6b. It reveals that the mass of adsorption increased with the increase of the initial concentration. The Langmuir adsorption model is used to represent the relationship between the amount of heavy metal adsorbed at equilibrium (q_e, mg g^{-1}) and the equilibrium solute concentration (C_e, mg L^{-1}):[50]

$$q_e = q_m b C_e/(1 + bC_e)$$

where q_m (mg g^{-1}) is the maximum sorption capacity corresponding to complete monolayer coverage and b is the equilibrium constant (L mg^{-1}). When such a model was adopted to analyze the adsorption isotherms, the maximum adsorption capacity (q_m) of the as-obtained ceria was found to be 14.4 mg g^{-1} for As(V) and 5.9 mg g^{-1} for Cr(VI). After the adsorption, the solid/liquid separation in suspension was rather easy by centrifugation as the as-prepared ceria was several micrometers in size. Thus, the ceria could be efficiently regenerated for recycle. When the used ceria was added to 50 mL of NaOH solution (0.2 mol L^{-1}) and then was stirred for 5 h and was centrifuged and washed with clean water, it was found that the regenerated ceria still kept high removal performance. For example, the removal capacity of the regenerated ceria for Cr(VI) was measured to be 3.3 mg g^{-1} when the initial concentration of Cr(VI) was 21.0 mg L^{-1}. For comparison, we investigated the removal capacity of a commercial ceria powder under the same experimental conditions. As shown in Figure S2, the size of the commercial ceria particles is ca. 1 μm and the surface is rather smooth. It was found that the removal capacity of this commercial ceria was 0.30 mg g^{-1} for As(V) and 0.37 mg g^{-1} for Cr(VI) when the initial concentration of As(V) and Cr(VI) was 39.2 and 21.0 mg L^{-1}, respectively. Obviously, the as-prepared ceria with 3D micro/nanocomposite structure shows much better removal capacity than the commercial ceria particles. The specific surface area was measured to be ca. 34.1 m^2 g^{-1} for the as-obtained ceria with micro/nanocomposite structure, much larger than that of the adopted commercial ceria particles (2.0 m^2 g^{-1}). The better performance for water treatment could be attributed to the porous structure and high specific surface area of the as-prepared ceria.

The removal of CO is also of fundamental importance in air purification, fuel cell, closed-cycle CO_2 laser, and many other applications. Since Haruta and co-workers discovered a remarkable catalysis activity of supported gold nanoparticles in CO oxidation,[51,52] strong interest in gold for catalyst emerged, and it had been found that highly dispersed gold nanoparticles on various oxides can catalyze CO oxidation.[53] Among the various reducible oxides, CeO_2 with the character of a high oxygen storage capacity had been used as support for gold catalyst and possessed unique properties.[19,47] Herein, Au nanoparticles were deposited on the as-obtained ceria by deposition−precipitation (DP) method, and the as-prepared Au/CeO_2 catalyst was used for CO catalytic oxidation. The total Au loading content of the Au/CeO_2 was 4.7 wt % as determined by inductively coupled plasma (ICP) test. Figure 7a shows the TEM analysis of the as-prepared

(48) Peng, X. J.; Luan, Z. K.; Ding, J.; Di, Z. H.; Li, Y. H.; Tian, B. H. *Mater. Lett.* **2005**, *59*, 399.
(49) Di, Z. C.; Ding, J.; Peng, X. J.; Li, Y. H.; Luan, Z. K.; Liang, J. *Chemosphere* **2006**, *62*, 861.
(50) Wu, R. C.; Qu, J. H.; Chen, Y. S. *Water Res.* **2005**, *39*, 630.
(51) Haruta, M.; Kobayashi, T.; Sano, H.; Yamada, N. *Chem. Lett.* **1987**, *16*, 405.
(52) Haruta, M.; Yamada, N.; Kobayashi, T.; Iijima, S. *J. Catal.* **1989**, *115*, 301.
(53) Daniel, M. C.; Astruc, D. *Chem. Rev.* **2004**, *104*, 293.

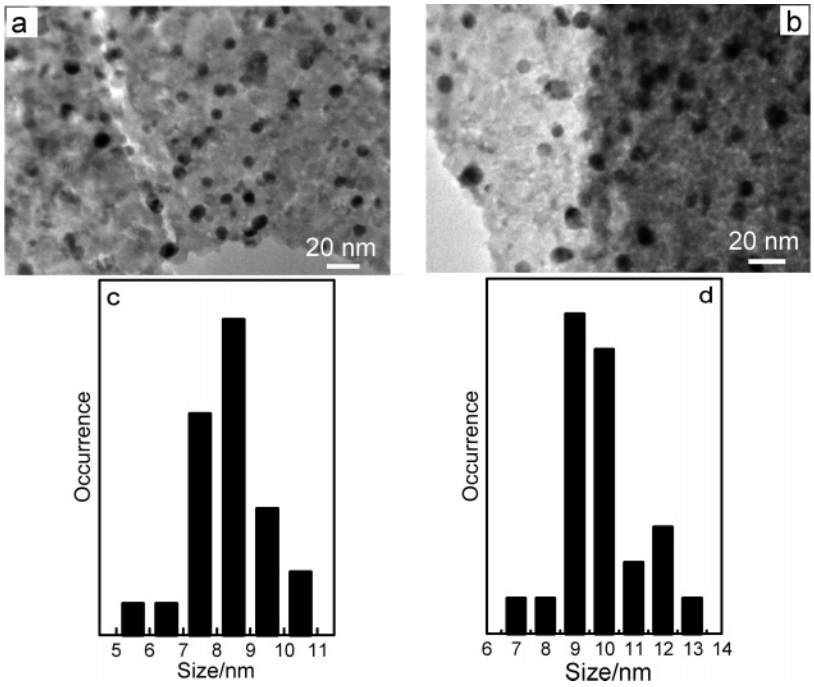

Figure 7. TEM images of the as-prepared Au/CeO_2 before (a) and after (b) catalysis. The size distribution of Au nanoparticles in Au/CeO_2 before (c) and after (d) catalysis.

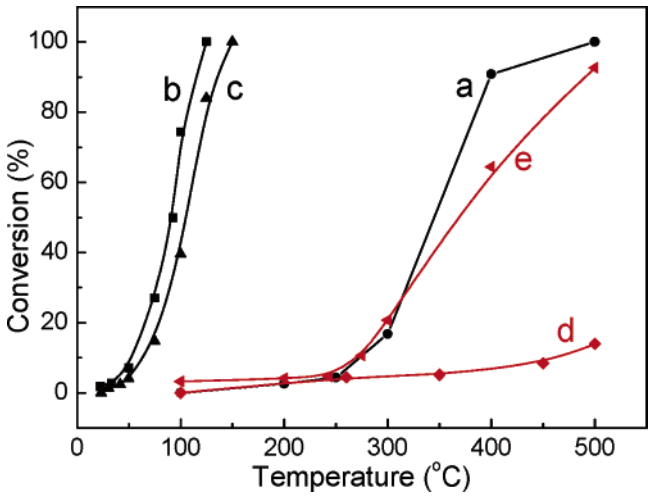

Figure 8. CO conversion as a function of temperature for the as-prepared CeO_2 (line a), new-prepared Au/CeO_2 (line b) catalyst, used Au/CeO_2 (line c), and commercial ceria powder without (line d) and with (line e) Au loading.

Au/CeO_2 catalyst by DP method. It is clear that Au nanoparticles (dark dots in the Figure 7a) were highly dispersed on the CeO_2 support with the mean diameter and the particle size distribution of 8.3 ± 1.1 nm (Figure 7c). In Figure 8, the CO conversion as a function of temperature is displayed for pure CeO_2 and Au/CeO_2 under the same experiment condition (line a and line b). The CO conversion increased with increasing reaction temperature for both samples and the synthesized Au/CeO_2 showed a higher catalytic activity than pure CeO_2. A 100% CO conversion was achieved at 125 °C for Au/CeO_2 while it needed 500 °C for the total conversion for pure CeO_2. Also, the half CO conversion temperatures for both samples were 90 °C for Au/CeO_2 and 350 °C for CeO_2. Obviously, the addition of Au nanoparticles significantly increased the catalytic activity of ceria. This could be attributed to the strong synergistic interaction between Au and CeO_2. CeO_2 supplied reactive oxygen by releasing−uptaking oxygen through redox process involving the Ce^{4+}/Ce^{3+} couple.[5] During the catalytic CO oxidation process, reactive oxygen from CeO_2 reacted with CO molecules adsorbed on Au nanoparticles to form CO_2.[47] To investigate the durability of the as-prepared Au/CeO_2 catalyst, another run was carried out after the catalyst had been continuously used for 10 h under the flow of mixture gas. As revealed by line c in Figure 8, the Au/CeO_2 still kept high catalytic activity for CO oxidation after 10 h of reaction time. To check for possible change of the catalyst, TEM was also performed to characterize the Au/CeO_2 after continuous reaction for 10 h. Figure 7b indicates that, after 10 h of reaction time, the Au nanoparticles still remained highly dispersed on the CeO_2 support and were not agglomerated. The mean diameter and the particle size distribution of Au nanoparticles were 9.8 ± 1.3 nm (Figure 7d), just lightly larger than before catalysis. The result indicated that the CeO_2 support with micro/nanocomposite structure could effectively stabilize the Au nanoparticles which made sure the as-prepared Au/CeO_2 catalyst had high catalytic activity and high durability. The commercial ceria particles with smooth surface were also used to test its ability for CO removal (line d and line e in Figure 8). As indicated by the results in Figure 8, the as-obtained ceria with 3D micro/nanocomposite structure shows much better performance for CO removal than the commercial ceria particles when either used as pure ceria or as a support for Au nanoparticles. The reason could also be due to highly porous structure and high specific surface area of the as-obtained ceria.

In addition, we also investigated the ability of ceria nanoparticles with a size of 10∼20 nm prepared by deposition method with $CeCl_3$ and NaOH solution (Figure S3). This kind of ceria nanoparticle is in higher specific surface area ($82.0\ m^2\ g^{-1}$) and shows better performance in water

treatment and CO removal than our ceria with 3D flowerlike micro/nanocomposite structure. However, the ceria with 3D flowerlike micro/nanocomposite structure is easier to be handled and recycled in the practical applications with the advantage of the nanoparticles as building blocks.

Conclusion

In summary, a simple and economical route based on ethylene glycol mediated self-assembly process was adopted to synthesize 3D flowerlike ceria micro/nanocomposite structure. A two-stage growth process was identified during the morphology evolution of ceria precursor. Ceria with the same flowerlike micro/nanocomposite structure was readily obtained by calcination from the ceria precursor. This novel micro/nanocomposite structure held the advantages of both microstructure and nanostructure. The as-obtained ceria was an effective sorbent for the removal of As(V) and Cr(VI) in water treatment. In addition, the as-obtained ceria could be acted as a support for gold nanoparticles and exhibited high activity for CO removal by catalytic oxidation with high durability. The as-obtained ceria should be a promising material for environmental application and is expected to be useful in many other application fields.

Acknowledgment. This work was partially supported by the National Natural Science Foundation of China (Nos. 20121301, 20603041, 20673121, and 20575070), the National Key Project on Basic Research (Nos. 2006CB806100), and the Chinese Academy of Sciences.

Supporting Information Available: SEM images of the ceria precursor prepared without the addition of TBAB and the used commercial ceria powder and TEM image of the ceria nanoparticles. This material is available free of charge via the Internet at http://pubs.acs.org.

CM062471B